Research article

Novel bioactive nanospheres show effective antibacterial effect against multiple endodontic pathogens

Jin Liu [a,b,1], Haoze Wu [a,1], Jun Qiu [a,1], Sirui Yang [a], Doudou Xiang [a], Xinhua Zhang [a], Jinxin Kuang [a], Min Xiao [a,**], Qing Yu [a,***], Xiaogang Cheng [a,*]

[a] State Key Laboratory of Oral & Maxillofacial Reconstruction and Regeneration, National Clinical Research Center for Oral Diseases, Shaanxi Key Laboratory of Stomatology, Department of Operative Dentistry and Endodontics, School of Stomatology, The Fourth Military Medical University, 145 West Chang-le Road, Xi'an, 710032, Shaanxi, PR China
[b] Department of Stomatology, Huangshan City People's Hospital, Huangshan, 245000, Anhui, PR China

ARTICLE INFO

ABSTRACT

Aim: The current study evaluated the antibacterial activity of a newly developed quaternary ammonium polymethacrylate (QAPM)-containing bioactive glasses (BGs) via a two-step method by our group, namely BGs-HAEMB, and explored its cytotoxicity and biocompatibility.
Methods: The antibacterial effects of the BGs-HAEMB against planktonic bacteria, bacterial bio-film formation, and experimental root canal biofilms of persistent pathogens (*Enterococcus faecalis*, *Streptococcus sanguis* and *Porphyromonas endodontalis*) associated with endodontic infection were evaluated *in vitro* by agar diffusion tests, direct contact tests and live/dead staining. The cytotoxicity and biocompatibility of BGs-HAEMB were evaluated by CCK-8 assays *in vitro* and a skin implantation model *in vivo*.
Results: Compared to three clinically used endodontic sealers (Endofill, AH Plus, and iRoot SP), BGs-HAEMB exhibited the relatively strongest antibacterial effect against *E. faecalis*, *S. sanguis* and *P. endodontalis* after sitting for 14 and 28 days ($P < 0.01$). SEM images and CLSM images also showed that for each tested bacteria, BGs-HAEMB killed the most microorganism among all the experimental groups, regardless of treatment for 7 days or 28 days ($P < 0.05$). Besides, the BGs-HAEMB-treated groups showed a relatively low cytotoxicity (RGRs ranging from 88.6% to 102.9%) after 1, 3, and 7 days of exposure. Meanwhile, after 28 days of implantation, the in-flammatory grade in BGs-HAEMB treated group was assessed as Grade I, in which the average numbers of inflammatory cells (6.7 ± 2.1) were less than 25.

* Corresponding author. State Key Laboratory of Oral & Maxillofacial Reconstruction and Regeneration, National Clinical Research Center for Oral Diseases, Shaanxi Key Laboratory of Stomatology, Department of Operative Dentistry and Endodontics, School of Stomatology, The Fourth Military Medical University, 145 West Chang-le Road, Xi'an, 710032, PR China.
** Corresponding author. State Key Laboratory of Oral & Maxillofacial Reconstruction and Regeneration, National Clinical Research Center for Oral Diseases, Shaanxi Key Laboratory of Stomatology, Department of Operative Dentistry and Endodontics, School of Stomatology, The Fourth Military Medical University, 145 West Chang-le Road, Xi'an, 710032, PR China.
*** Corresponding author. State Key Laboratory of Oral & Maxillofacial Reconstruction and Regeneration, National Clinical Research Center for Oral Diseases, Shaanxi Key Laboratory of Stomatology, Department of Operative Dentistry and Endodontics, School of Stomatology, The Fourth Military Medical University, 145 West Chang-le Road, Xi'an, 710032, PR China.
E-mail addresses: 2276548842@qq.com (J. Liu), wuhaoze0830@163.com (H. Wu), qiujun@fmmu.edu.cn (J. Qiu), 2046460187@qq.com (S. Yang), xiangdoudou163@163.com (D. Xiang), 2594318790@qq.com (X. Zhang), kuangjinxin96@outlook.com (J. Kuang), 598188739@qq.com (M. Xiao), yuqing@fmmu.edu.cn (Q. Yu), chengxg5410@163.com (X. Cheng).
[1] These authors contributed equally to this work.

Conclusions: BGs-HAEMB exerted a long-term and stable antibacterial effect. The remarkable biocompatibility of BGs-HAEMB *in vitro* and *in vivo* confirmed its possible clinical application as a potential alternative in the development of the next generation of endodontic sealers.

1. Introduction

Endodontic diseases are among the most common oral diseases and are mainly initiated by oral microbial infections and are closely associated with multiple risk factors [1]. Endodontic diseases often can cause orofacial pain, considerable discomfort, and ultimately tooth loss [2]. It has also been documented that these diseases may act as focal infections that are closely associated with systemic diseases such as diabetes, hypertension, and coronary heart disease [3].

Root canal therapy (RCT) is applied as the first strategy in the management of endodontic diseases [4]. Thorough elimination of root canal infection, which is accomplished through root canal cleaning, shaping, disinfection, and filling, is the key for the success of RCT [5]. However, due to the anatomy and infection complexity of the root canal system, it is virtually impossible for conventional chemo-mechanical procedures to completely eradicate infections within a tooth root. Residual bacteria can cause reinfection, leading to RCT failure [6]. *Enterococcus faecalis* (*E. faecalis*) is the main species isolated from an endodontically treated root canals with posttreatment endodontic diseases [7]. *E. faecalis* secrete various virulence factors, such as collagen-binding proteins, gelatinase, and surface proteins, and mediate bacterial biofilm formation, resulting in drug resistance and microorganism survival in complex root canal systems [8]. In addition, high levels of *Streptococcus sanguis* (*S. sanguis*) and *Porphyromonas endodontalis* (*P. endodontalis*) have also been detected at apical lesions in patients with periapical diseases and play an important role in the development of endodontic diseases by inducing virulence factors and stimulating the progression of osteoclastogenesis [9]. As the final step in RCT, the root canal system is filled with a core bioinert material (e.g., gutta percha) combined with an endodontic sealer [10]. Therefore, it is desirable for the endodontic sealer to exhibit antibacterial activity to restrain the growth of the residual bacteria that were not affected by chemo-mechanical procedures.

However, there is still a great gap in the ability of current commercial endodontic sealers to exhibit satisfactory antibacterial activity. For example, Endofill, a zinc oxide and eugenol-based sealer with dimensional stability and high solubility, also shows antibacterial activity. However, its high solubility acts as a double-edged sword in terms of its apical sealing ability [11]. AH Plus, an epoxy resin-based sealer, is one of the most used endodontic sealers during RCT. It can adhere to dentine and shows antibacterial effects against *E. faecalis*. AH Plus also exhibits relatively good biocompatibility and long-term structural stability [12]. However, it has several limitations, such as cytotoxicity, no potential for bioactivity, and possible mutagenicity, and it may also induce inflammation [13]. iRoot SP, a ready-to-use nanobioceramic material, is another commonly used sealer during endodontic treatment. It possesses superior biocompatibility, osteogenic potential and marked apical sealing ability, along with persistent antibacterial effects against *E. faecalis* [14,15]. However, its significant reductions in setting time and flow at high temperatures and may lead to poor quality obturation during root canal filling when using warm vertical compaction [16]. In addition, the tooth discoloration caused by iRoot SP and its mild cytotoxicity further limit its use as an endodontic sealer [17]. Therefore, developing promising adjuvants with better antibacterial effects and prolonged efficacy but fewer side effects compared to current commercial endodontic sealers is greatly needed.

Various materials have shown remarkable antibacterial effects against endodontic pathogens [18,19]. Previous studies found a material called bioactive glass (BG) with good osteogenic, angiogenic, and antibacterial abilities and biosafety [20–22]. BGs are mainly used to increase bone mass, especially alveolar bone mass, and are widely used during periodontal therapy [23,24]. In previous studies, BGs were reported to be carriers of calcium, phosphate, and silica to enhance mineral precipitation in dentinal tubules, showing an effect in the treatment of dentinal hypersensitivity [25]. In addition, BGs show superior antibacterial activity in dentinal tubules due to the complex ionic reaction between the BGs and dentine in the root canal [26,27]. Quaternary ammonium methacrylate salt (QAM) polymers, a kind of polyelectrolyte containing QAM groups, have been used as medical bactericides or daily chemical agents due to their good water solubility, high efficiency, nontoxicity, and adjustable cationicity and molecular weight [28,29]. Recent studies have demonstrated that QAM monomers in covalently modifying resin materials can not only maintain the original mechanical properties of the composite materials but also cause new materials to display stable contact antibacterial effects [30]. Given the broad antimicrobial spectrum, antifungal effects, and low cytotoxicity of QAMs when treating oral bacteria, QAMs have been widely used in the oral cavity [31].

In this study, we synthesized BGs by using a sol-gel method for modification with QAMs by using a two-step coupling method. Quaternary ammonium polymethacrylate (QAPM)-containing bioactive glasses, named BGs-HAEMB, were generated successfully. The characterization of BGs-HAEMB was analyzed and verified by using scanning electron microscopy (SEM), transmission electron microscopy (TEM), energy dispersive X-ray spectroscopy (EDS), and Fourier transform infrared (FTIR) spectroscopy. Compared to three currently used endodontic sealers (Endofill, AH Plus, and iRoot SP), both *in vitro* and *in vivo* studies revealed that BGs-HAEMB possessed a more effective, long-term, and stable antibacterial activity against *E. faecalis*, *S. sanguis* and *P. endodontalis*, as well as a relatively lower cytotoxicity and better biocompatibility, representing its great potential in the development of the next generation of endodontic sealers.

2. Materials and methods

2.1. Bacterial preparation and growth conditions

E. faecalis (ATCC 29212), *S. sanguis* (ATCC 10556), and *P. endodontalis* (ATCC 35406) were obtained from the State Key Laboratory of Military Stomatology (the School of Stomatology, the Fourth Military Medical University, Xi'an, China). *E. faecalis*, *S. sanguis* and *P. endodontalis* were routinely cultured in brain heart infusion broth (BHI broth, Difco, Sparks, MD) at 37 °C under anaerobic conditions.

2.2. Materials

Ammonia water, cetyltrimethylammonium bromide (CTAB), triethyl phosphate (TEP), tetrahydrate calcium nitrate (CN), tetraethyl orthosilicate (TEOS), anhydrous ethanol, 2-(dimethylamino) ethyl methacrylate (DMAEMA), 1-bromopropane (BP), 1-bromononane (BN), 1-bromohexadecane (BHD), 1-bromooctadecane (BOD), benzoyl peroxide (BPO), deionized water (DW), and KH-570 were all purchased from Sigma–Aldrich (Darmstadt, Germany).

2.3. BG synthesis and characterization

2.3.1. Synthesis of the BG

Solution A was prepared by mixing 200 mL of sterile water with 9 mL of ammonia water and 0.6 g of CTAB using a magnetic stirrer. Pre-dissolved inorganic molecules (186 μL of TEP in 1 mL of anhydrous ethanol, 0.78 g of CN in 1 mL DW, and 3.9 mL of TEOS in 1 mL of anhydrous ethanol) were slowly added to solution A at intervals of 30 min. After overnight stirring, the clear solution turned milky white. This solution was centrifuged at 8000 rpm, and the supernatant was discarded. The obtained precipitate was washed alternately with anhydrous ethanol and DW. After drying, the precipitate was sintered at 600 °C for 4 h to obtain the BG. Moreover, different volumes (7.8 mL, 15.6 mL) of TEOS were added to synthesize BGs with different particle sizes.

2.3.2. Characterization of the BGs

The BGs was mixed with sterile water, and 10 μL of the solution was placed on a silicon wafer and carbon film after 30 s of ultrasonic crushing. After drying, the BGs were observed using SEM (Hitachi, Japan) and TEM (Thermo Fisher Scientific, USA).

2.4. Synthesis and characterization of the QAMs

2.4.1. Synthesis of the QAMs

QAM monomers with different nitrogen alkyl chain lengths (N-ACLs) were synthesized via an addition reaction. The procedure described below is based on the synthesis of propyldimethyl ammonium ethylmethacrylate bromide (PAEMB, N-ACL = 3). In brief, anhydrous ethanol (5 mL), DMAEMA (17.5 mmol), and BP (17.5 mmol) were added to a vial and mixed with continuous magnetic stirring for 24 h in a silicone oil bath at 75 °C. The product was freeze-dried at −60 °C for 48 h to obtain PAEMB. In addition, QAM monomers with different N-ACLs of 9, 16, and 18 were also synthesized using BN, BHD, and BOD, respectively, and denoted as NAEMB, HAEMB, and OAEMB.

2.4.2. Characterization of the QAMs

2.4.2.1. Nuclear magnetic resonance (NMR) measurements. Deuterated chloroform was used as the solvent and mixed with the four kinds of QAMs. The purities of the products were evaluated by measuring the intensity of the characteristic peak of the H atom at the different positions of the QAMs.

2.4.2.2. FTIR. QAM (1 mg) and KBr (0.1 g) were mixed, laminated, and placed inside the instrument. The range of 4000 to 500 cm^{-1} was scanned at a resolution of 0.09 cm^{-1}.

2.4.2.3. EDS. Appropriate amounts of the four types of QAMs were placed on a conductive adhesive, compacted, and placed on a stage. The stage was placed inside the energy dispersive X-ray spectroscopy (EDS) instrument with SEM for elemental analysis.

2.4.2.4. Minimum inhibitory concentrations (MICs) and minimum bactericidal concentrations (MBCs) of the QAMs. PAEMB, NAEMB, HAEMB, and OAEMB were mixed with BHI broth, and the initial concentrations were adjusted to 3.2 g/mL, 0.04 g/mL, 200 μg/mL, and 200 μg/mL, respectively. Each solution was filtered with a 0.22-μm filter.

The antibacterial activity of the QAMs against pathogens (*E. faecalis*, *S. sanguis*, and *P. endodontalis*) was determined by the microdilution method. The procedure is described using PAEMB as the representative example. The final concentrations of PAEMB were adjusted from 3.2 g/mL to 3.125×10^{-3} g/mL in 2-fold serial dilutions with BHI broth. 100 μL of each diluted solution were added to different wells of a 96-well plate. 100 μL of bacterial suspension with final concentration of 10^6 CFU/mL was added to the QAM solution. Equal volumes of bacterial solution without QAM solution were used as the negative control and BHI broth without

bacteria but with QAM solution as the blank control. The plate was incubated anaerobically for 24 h, and the MIC was defined as the lowest concentration of the agent that showed no visible bacterial growth. To determine the MBC, 100 μL of clear bacterial cultures were added to BHI agar plates and incubated for 48 h. The lowest concentration of the agent that completely inhibited bacterial growth was considered the MBC. The MICs and MBCs of NAEMB, HAEMB, and OAEMB were determined in the same way.

2.5. Synthesis of BGs-HAEMB

The synthesis process of BGs-HAEMB is shown in Fig. 1A briefly.

(1) The entire experiment was conducted under nitrogen protection. Toluene was added to a flask and heated. Sodium metal was cut into thin strips and added to the above flask with a small amount of benzophenone. The successful removal of water was indicated by a change in the color of benzophenone.
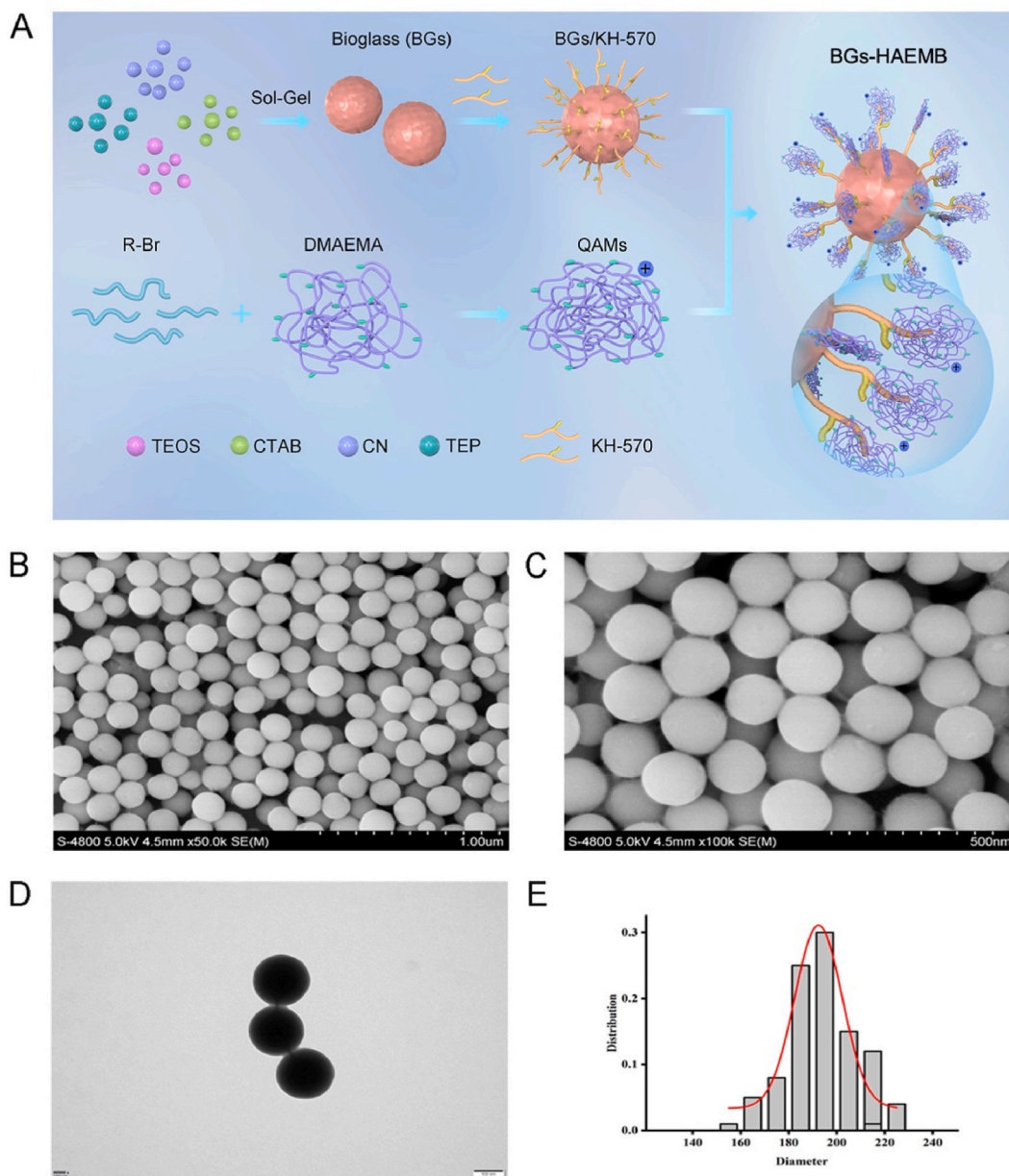

Fig. 1. (A) Schematic diagram of the synthesis of BGs-HAEMB. (B, C) SEM images of BGs-HAEMB. (D) TEM images of BGs-HAEMB. (E) Size distribution histogram of the BGs-HAEMB.

(2) BGs (5 g, 181 nm) was added to anhydrous toluene and dispersed using ultrasound. After adding 10 mL of KH-570, the mixture was placed in a 150 °C silicone oil bath and stirred magnetically for 24 h to successfully carry out the grafting reaction.

The material obtained after the reaction was centrifuged. The product was rinsed repeatedly with ethanol and DW, and the final product was collected after freeze drying. This product was labeled as BGs/KH-570.

(3) The BGs/KH-570 (10 g) was dissolved in 100 mL of 1-butanol, and the solution obtained after ultrasound was denoted as solution A.
(4) HAEMB (10 g) and BPO (100 mg) were dispersed in 50 mL of 1-butanol to obtain solution B.
(5) Solutions A and B were mixed and reacted in a silicone oil bath at 80 °C for 24 h. The mixture was centrifuged to collect the final product. The crude products were rinsed with ethanol and DW and freeze-dried to obtain BGs-HAEMB.

2.6. Characterization of BGs-HAEMB

Characterization procedures of BGs-HAEMB are similar to that of BGs and QAMs. SEM and TEM were used to observe the morphology of BGs-HAEMB, and the EDS and FTIR were taken as described above.

2.7. Test materials

BGs-HAEMB was dissolved in sterile water after disinfection. Three commercial endodontic sealers, Endofill (Dentsply, Brazil), AH Plus (Dentsply DeTrey, Konstanz, Germany), and iRoot SP (Innovative BioCeramix Inc., Canada) were prepared following the manufacturers' instructions.

2.8. Evaluation of the antibacterial effects of BGs-HAEMB

2.8.1. Effects of BGs-HAEMB on planktonic bacteria

2.8.1.1. Agar diffusion test (ADT). 200 μL of *E. faecalis*, *S. sanguis*, and *P. endodontalis* were spread on BHI agar plates, and the plates were evenly coated and naturally dried. Holes (5 mm in diameter, 4 mm in height) were punched into the agar to accommodate the test materials (20 mg per group). Ampicillin (10 μg, Honsun, China) served as the positive control [32], whereas sterile water served as the negative control. After placing at room temperature for 2 h, the plates were incubated at 37 °C for 24–48 h. The diameter of the effective bacteriostatic ring was measured and defined as the average value of the diameter of the bacteriostatic ring in the vertical direction minus the distance of the aperture.

2.8.1.2. Direct contact test (DCT). The test materials (30 μg) were coated onto the sidewall of a 96-well plate and cured at 37 °C for 20 min (fresh) and 1, 7, 14, and 28 days. The 96-well plates were removed at preset time points, and 10 μL of bacterial solution (1×10^8 CFU/mL) was added to the surface of the materials after exposure to ultraviolet radiation for 2 h. After continuous contact for 60 min, 240 μL of BHI medium was added for 24 h of culture. Bacteria grown without the material was used as a negative control and BHI alone as blank control. Then, 100 μL of gradient dilutions of bacterial solutions were plated on BHI agar and incubated for 48 h, and the number of colonies was counted. The total number of colonies was calculated as the number of CFU multiplied by the dilution ratio.

2.8.2. Determination of the inhibitory effects of BGs-HAEMB on biofilm formation in vitro

E. faecalis, *S. sanguis* and *P. endodontalis* were grown on the surface of different test materials. In brief, sterile polyethylene tube molds (8 mm in diameter, 1 mm in height) were placed on cover glasses (Fisher, USA), and the tested materials were placed in the mold and cured for 20 min and 1, 7, 14, and 28 days. At each time point, the excess material on the surface was scraped off, the molds were removed, and the materials were placed in 6-well plates and exposed to ultraviolet radiation for 2 h. After that, suspensions of different bacteria (3 mL, 1×10^5 CFU/mL) were added, and the plates were incubated for 72 h. After incubation, the supernatant in each well was removed, and the adherent biofilm was washed twice with phosphate-buffered saline (PBS) to remove the planktonic cells.

For live/dead imaging, biofilms were stained with bacterial dye (Invitrogen, USA). Green fluorescence represented living bacteria, while red fluorescence represented dead bacteria. The dyed biofilms were observed and imaged with a confocal laser scanning microscopy (CLSM, Olympus, Japan), and the fluorescence intensity in the different groups were analyzed by Imaris 9.0 software (Bitplane, Zürich, Switzerland) to compare the antibacterial effects.

2.8.3. Antibacterial activity of BGs-HAEMB against bacterial biofilm formation in experimental dentinal tubules in vitro

Single-rooted teeth extracted due to orthodontic treatments were collected with approval by the Ethics Committee of the School of Stomatology, the Fourth Military Medical University (IRB-REV-2018013). The dentinal specimens were prepared as described previously with minor modifications [33]. In brief, the dental calculus and soft tissues were removed from 160 collected teeth, and the tooth crowns were removed by using a slow cutting saw. The root dentin blocks (5 mm in length, 320 were acquired in total) were obtained from the remaining roots with a diamond-coated saw. The medullary cavity inside the blocks was trimmed with a Gate-Glidden bur (#5, MANI, Japan) and then washed with alternate cycles of 5.25% NaClO and 17% EDTA. After sterilized at 121 °C

for 30 min, five randomly selected dentin blocks were subjected to BHI broth under anaerobic conditions at 37 °C for 48 h to ensure that the specimens were not contaminated.

The remaining 315 dentin blocks were then divided into 3 groups (n = 105) and placed on the bottom of 12-well plates (one per well) for *E. faecalis*, *S. sanguis*, and *P. endodontalis* contamination. BHI broth (1.8 mL) and bacterial suspensions (200 μL, 1×10^8 CFU/mL) were added to each well, and the plates were incubated for 28 days. The BHI medium was refreshed every other day. After 28 days of incubation, five randomly selected samples from each group were examined by SEM to ensure bacterial colonization after inoculation.

Specimens were then dried with sterile paper points. For each test strain, the remaining 100 samples were randomly divided into five groups (n = 20). After the materials (Endofill, AH Plus, iRoot SP, and BGs-HAEMB) were coated onto the surfaces of the root canal walls and compacted, the samples were then placed in 12-well plates and cultured for 7 and 28 days at 100% relative humidity and 37 °C. Sterile normal saline was used as the negative control. At each time point, 10 specimens from each material group were divided into two subgroups. One subgroup (n = 6) was ground with a Gate-Glidden bur (#6) to collect dentin debris, mixed with BHI broth, and then cultured on an agar plate for colony counting. The specimens in the other subgroup (n = 4) were split into two halves. One half was used for live/dead staining, imaging and observation by CLSM. The proportion of dead bacteria inside the dentinal tubules was calculated according to the following formula: ratio of dead bacteria (%) = V (red fluorescence)/V (red fluorescence + green fluorescence) × 100%.

The other half of the samples was fixed, dried, sprayed with gold and observed via SEM.

2.9. Evaluation of the cytotoxicity of BGs-HAEMB

The cytotoxicity of the test materials was evaluated by Cell Counting Kit-8 (CCK-8, Dojindo, Kumamoto, Japan). Each material was shaped into discs with a diameter of 8 mm and height of 1.5 mm for extract preparation. After curing, the materials were exposed to ultraviolet radiation for 2 h and then placed in 1 mL of MEM (Gibco, USA) supplemented with 10% fetal bovine serum (FBS, Gibco, USA). The medium was incubated at 37 °C in a constant temperature oscillator for 24 h, and the supernatant was collected and sterilized using a 0.22-μm filter for further experiments.

Thawed L929 cells provided by the State Key Laboratory of Military Stomatology (the School of Stomatology, the Fourth Military Medical University) were cultured in MEM containing 10% fetal bovine serum and 1% penicillin−streptomycin (Invitrogen, USA) at 37 °C in a humidified atmosphere containing 5% CO_2. 200 μL of cell suspension with a final density of 1×10^4 per well was inoculated into 96-well plates for 24 h. Then, the culture medium was removed, and 200 μL of the extracts were added. Cell culture medium without extract was used as a negative control. The medium was changed every two days. 10 μL of CCK-8 solution were added to each well on days 1, 3, and 7. After incubation at 37 °C for 2 h, the absorbance of each sample was measured at 450 nm by a microplate reader (BIO-TEX, USA). The relative growth rate (RGR) of the cells = $OD_{\text{mean value of the experimental control}}/OD_{\text{mean value of the negative group}} \times$ 100%. RGR grades were assigned as follows: Grade 0, RGR ≥100%; Grade 1, 75% ≤ RGR <100%; Grade 2, 50% ≤ RGR <75%; Grade 3, 25% ≤ RGR <50%, Grade 4, 1% ≤ RGR <25%, and Grade 5, RGR <1%. Grade 0/1 was defined as qualified according to the corresponding standard (GB/T16886.5-2003) [34].

2.10. Evaluation of the biocompatibility of BGs-HAEMB in vivo

2.10.1. Experimental protocol

To prepare the implantation modules, BGs-HAEMB, Endofill, AH Plus and iRoot SP were filled and compacted into sterile polyethylene pipes with a length of 10 mm and an internal diameter of 1 mm. Blank polyethylene tubes were used as controls.

To evaluate biocompatibility, twenty Sprague−Dawley rats (8 weeks old, male, 250 g–300 g) acquired from the Animal Center of the School of Stomatology, the Fourth Military Medical University, were used. The experimental protocols were approved by the Ethics Committee of the school (IRB-REV-2018013). The rats were anesthetized with 0.1% pentobarbital sodium (0.6 mL/100 g i. p.). After removing their back hair and disinfecting, a crossing incision was made on the back skin, and the soft tissue was bluntly separated for material implantation. The freshly prepared BGs-HAEMB, Endofill, AH Plus and iRoot SP modules were carefully and randomly implanted into the pre-separated capsule cavity, and the control module was also implanted in the center of the operation area, opposite from the incision lines. The wounds were sutured with 5–0 sutures. The diet and behavior of the rats and postoperative complications were observed. At designated time points (7 and 28 days), rats (n = 10) were sacrificed using excessive anesthesia. The modules and surrounding tissues were collected, fixed and embedded. The embedded tissues were sliced and stained with hematoxylin and eosin (H&E, Solarbio).

The inflammatory reaction in the tissues was observed via microscopy, and the numbers of inflammatory cells, such as neutrophils, plasma cells, and lymphocytes, were calculated and analyzed. The inflammatory grades were determined as follows [35]: Grade I: no or low inflammatory response with <25 inflammatory cells; Grade II: moderate inflammatory response with <125 inflammatory cells; Grade III: severe inflammatory response with a large number of inflammatory cells (≥125) and a disordered tissue structure.

2.11. Statistical analysis

Every experiment was conducted in triplicate and the data are presented as the mean ± standard deviation (SD). Statistical analyses were performed with SPSS 22.0 software (SPSS Inc., Chicago, IL, USA). Multiple group comparisons were performed by one-way analysis of variance followed by Tukey's test to compare differences between groups, and two-group comparisons were performed by unpaired Student's *t*-test. The data were considered statistically significant at a *P* value of <0.05.

3. Results

3.1. Characterization of the BGs

The BG particles exhibited a regular and smooth spherical morphology with uniform size and texture and did not obviously aggregate (Figs. S1A–I). Furthermore, the average diameter of the BGs increased when the volume of TEOS increased (Fig. S1J–L). The EDS analysis was showed in Fig. S3 that the BGs were composed of elements Si, Ca, P, and O. The relative intensity of the peaks indicated the molar ratio of SiO_2: CaO: P_2O_5 was approximately 82 : 13 : 5 (unprovided data).

A Average diameter of the bacteriostatic rings of the tested materials against *E. faecalis*, *S. sanguis* and *P. endodontalis* ($\bar{x} \pm s$)

Bacterial species	Endofill	AH Plus	iRoot SP	Ampicillin	BGs-HAEMB	Sterile water
E. faecalis	4.74 ± 0.25^a	3.83 ± 0.17^b	0^c	24.38 ± 0.68^d	0^c	0^e
S. sanguis	18.28 ± 0.54^a	9.35 ± 0.41^b	0^c	34.35 ± 1.16^d	0^c	0^e
P. endodontalis	26.58 ± 0.86^a	3.94 ± 0.15^b	0^c	18.24 ± 1.05^d	0^c	0^e

B *E.faecalis*   *S.sanguis*   *P.endodontalis*

C control iRoot SP AH Plus Endofill BGs-HAEMB

LogCFU/mL

E.faecalis   *S.sanguis*   *P.endodontalis*
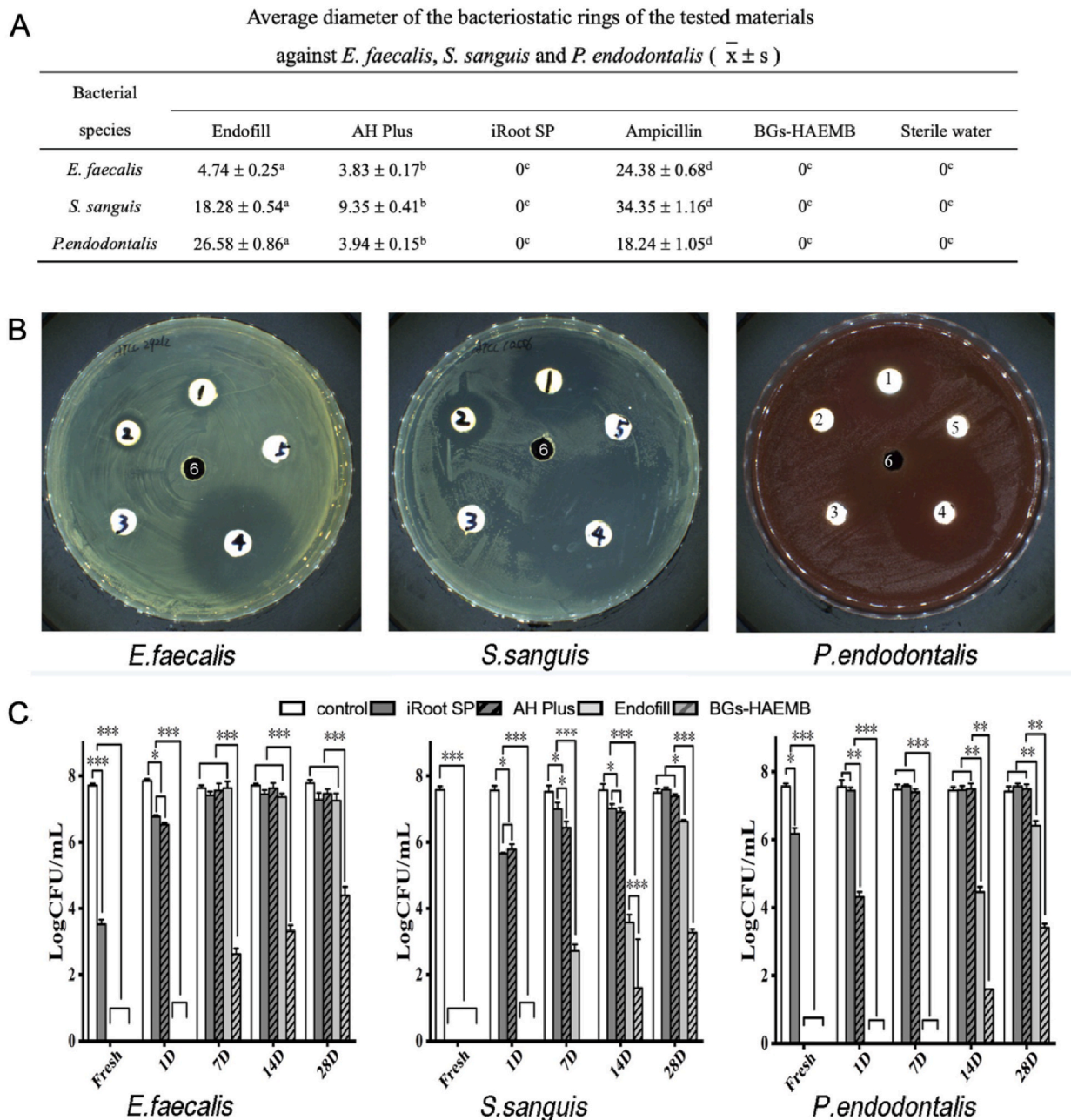
Fresh 1D 7D 14D 28D

Fig. 2. Antibacterial effects of BGs-HAEMB, Endofill, AH Plus, and iRoot SPagainst *E. faecalis*, *S. sanguis* and *P. endodontalis*. (A) Average diameters of the bacteriostatic rings of the tested materials against *E. faecalis*, *S. sanguis* and *P. endodontalis* ($\bar{x} \pm s$). [a-d] Comparisons of different labeled groups were statistically significant for the specific bacterial strain. (B) Representative images of bacteriostatic rings of Endofill (1), AH Plus (2), iRoot SP (3), ampicillin (4), BGs-HAEMB (5) and sterile water (6) against *E. faecalis*, *S. sanguis* and *P. endodontalis*. (C). Viable bacterial count of *E. faecalis*, *S. sanguis* and *P. endodontalis* treated by Endofill, AH Plus, iRoot SP and BGs-HAEMB of different sitting times. $^*P < 0.05, ^{**}P < 0.01$.

3.2. Characterization of the QAMs

Four types of QAMs (PAEMB, NAEMB, HAEMB, OAEMB) were successfully synthesized. Figs. S2A–D shows the NMR spectra of the different QAMs. Consistent with the NMR results, the EDS mapping results indicated that the mass of C also increased with increasing N-ACL (Figs. S2E–H). In addition, as shown in the ATR-FTIR spectra (Fig. S2I), the characteristic C–H stretching peak was observed at
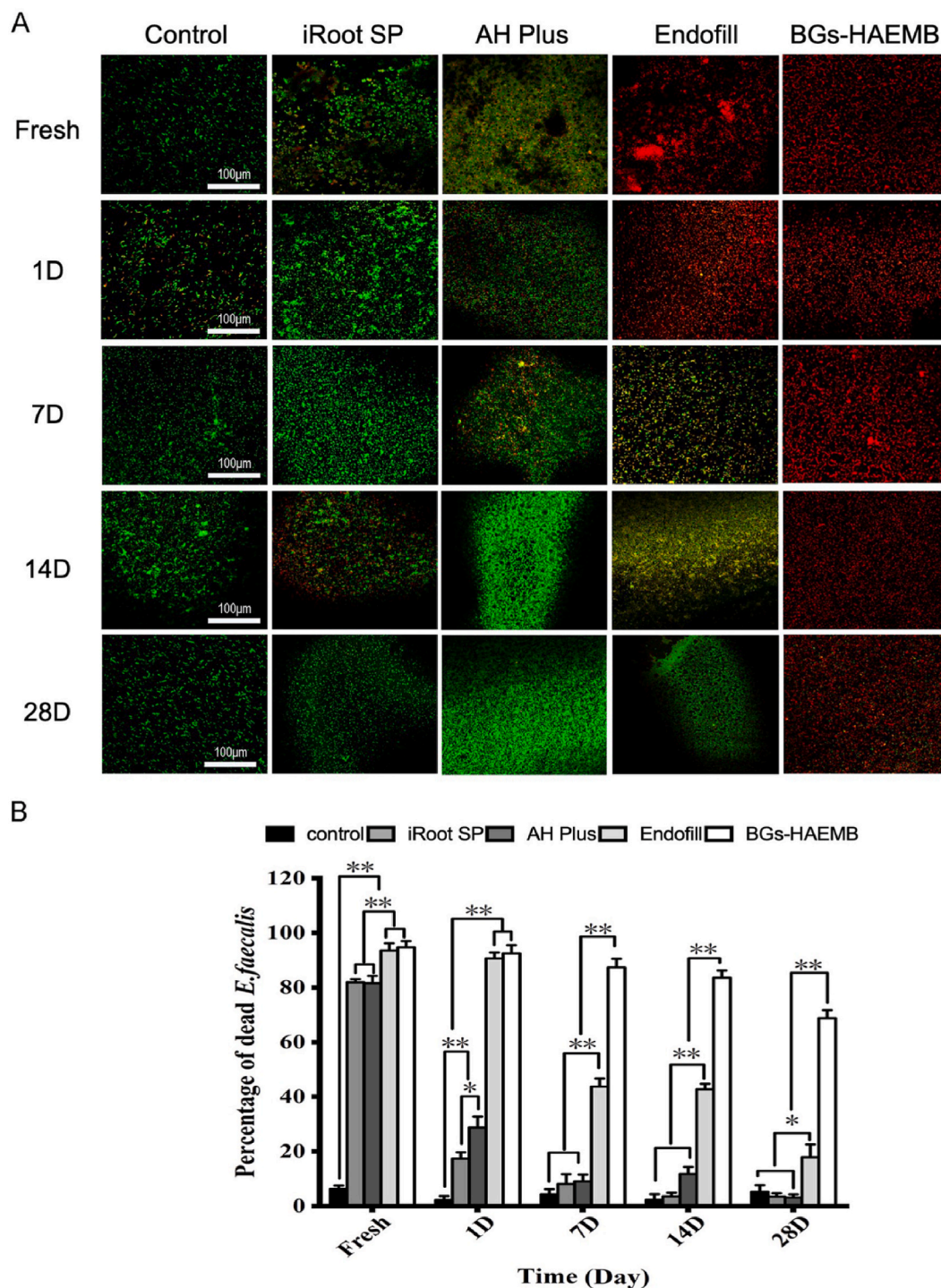

Fig. 3. Inhibitory effect of BGs-HAEMB, Endofill, AH Plus and iRoot SP against *E. faecalis* biofilm formation. (A) Representative images of dead/live bacteria staining of *E. faecalis* (Scale bar: 100 μm). (B) Quantitative analysis of the dead bacteria ratio within the biofilms, $^{*}P < 0.05,^{**}P < 0.01$.

2800 to 2900 cm^{-1}. The intensity of the C–H peak increased as the N-ACL in the QAMs increased.

3.3. Antibacterial activity of the QAMs

The MICs and MBCs of the four QAMs against *E. faecalis*, *S. sanguinis*, and *P. endodontalis* were determined and listed in Table S1. HAEMB (N-ACL = 16) showed the strongest antibacterial activity among all the QAMs. The MICs of HAEMB against *E. faecalis* and
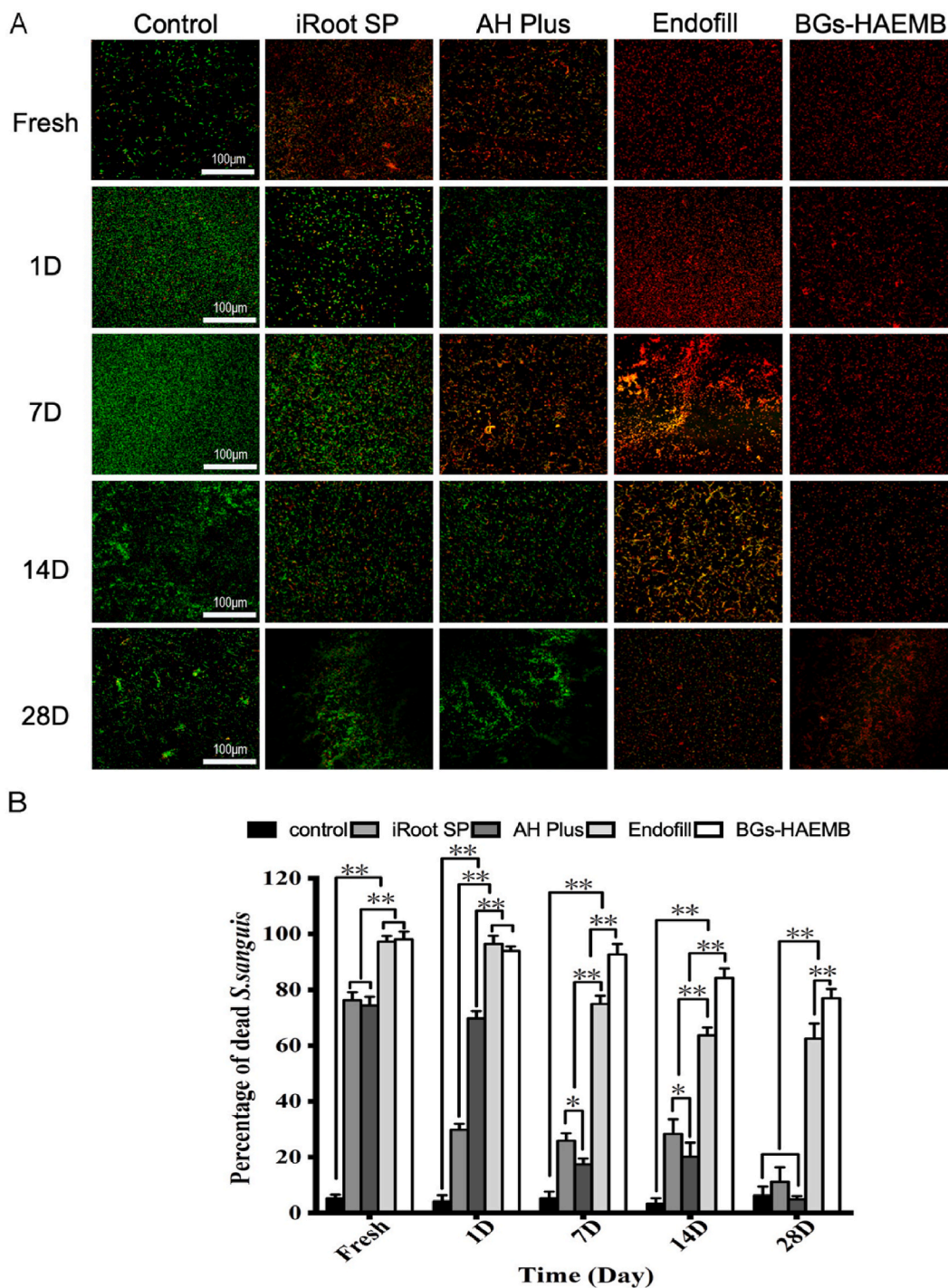

Fig. 4. Inhibitory effect of BGs-HAEMB, Endofill, AH Plus and iRoot SP against *S. sanguis* biofilm formation. (A) Representative images of dead/live bacteria staining of *S. sanguis* (Scale bar: 100 μm). (B) Quantitative analysis of the dead bacteria ratio within the biofilms, $^*P < 0.05, ^{**}P < 0.01$.
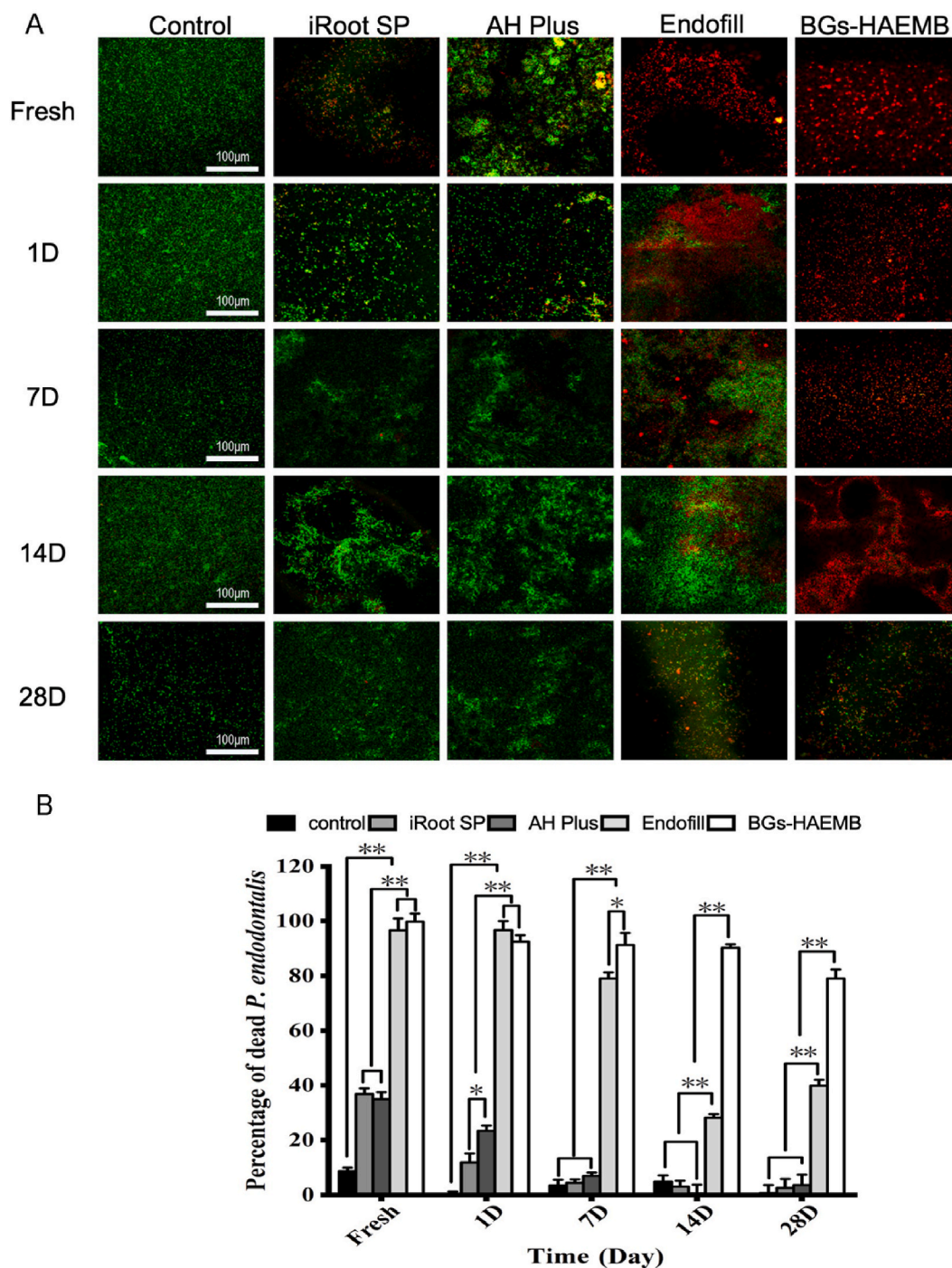
Fig. 5. Inhibitory effect of BGs-HAEMB, Endofill, AH Plus and iRoot SP against *P. endodontalis* biofilm formation. (A) Representative images of dead/live bacteria staining of *P. endodontalis* (Scale bar: 100 μm). (B) Quantitative analysis of the dead bacteria ratio within the biofilms, $^{*}P < 0.05, ^{**}P < 0.01$.
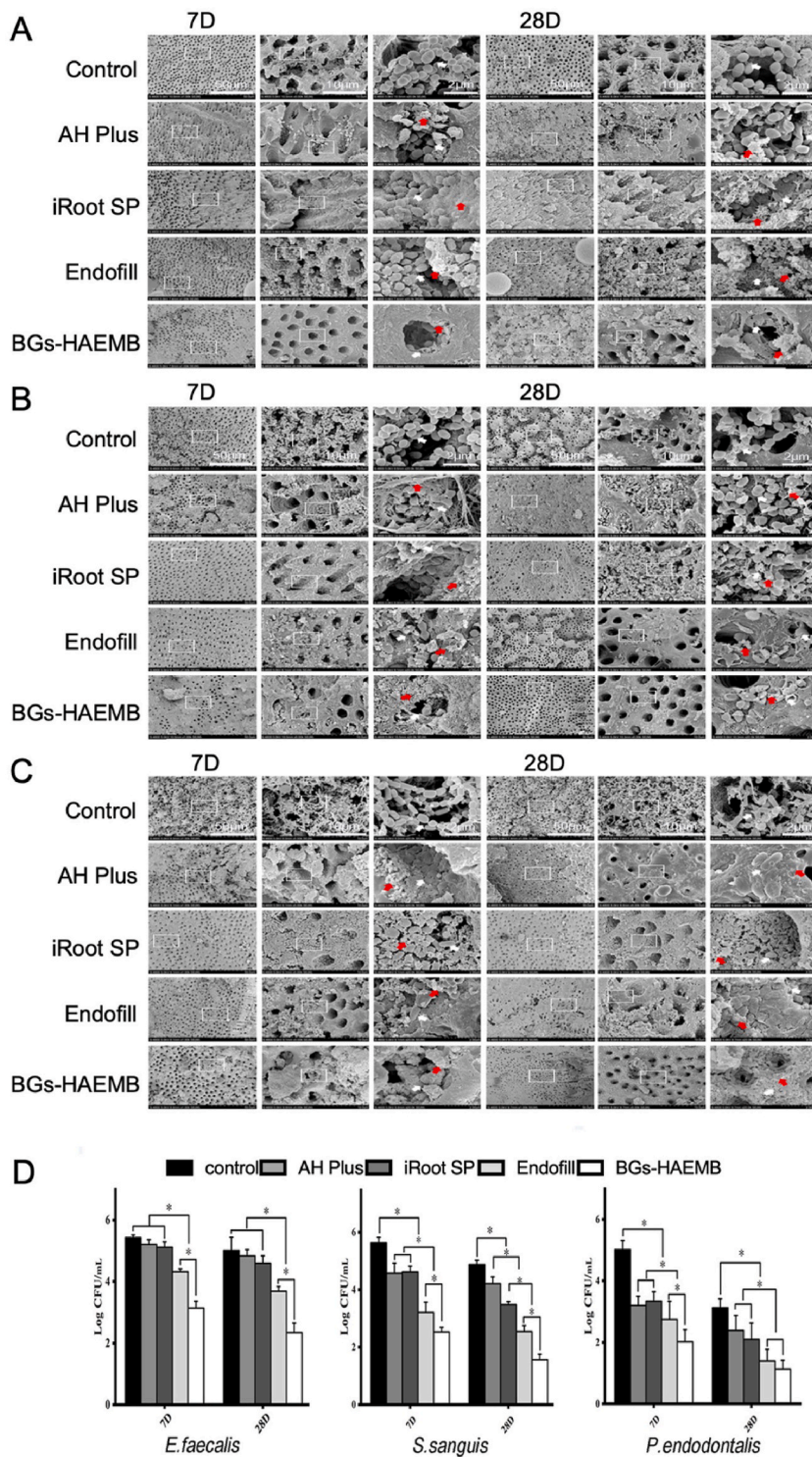
Fig. 6. The 7-days and 28-days antibacterial effects of BGs-HAEMB, Endofill, AH Plus and iRoot SP against *E. faecalis*, *S. sanguis* and *P. endodontalis*. (A) *E. faecalis* biofilms after treatment; (B) *S. sanguis* biofilms after treatment; (C) *P. endodontalis* biofilms after treatment; (D) Quantitative analysis of the antibacterial effects of experimental materials on *E. faecalis*, *S. sanguis* and *P. endodontalis* biofilms in experimental root canals. The white arrow indicates bacteria; the red arrow indicates the materials. $^*P < 0.05$. (For interpretation of the references to color in this figure legend, the reader is referred to the Web version of this article.)

A

B
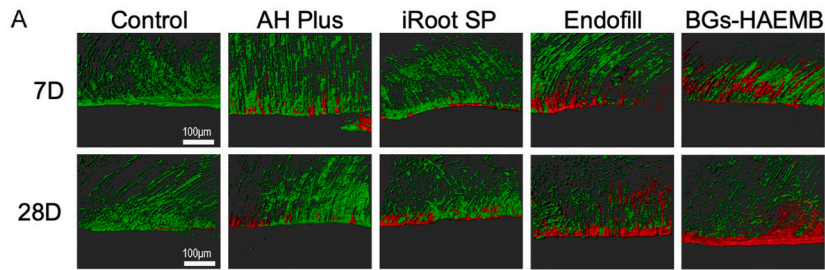
Materials	Red fluorescence ratio of *E. faecalis* at 7 and 28 days treatment ($\bar{x} \pm s$)	
	Time (Day)	
	7D	28D
Control	0.04 ± 0.03^a	0.07 ± 0.05^a
AH Plus	0.08 ± 0.02^a	0.12 ± 0.04^b
iRoot SP	0.07 ± 0.05^a	0.18 ± 0.02^b
Endofill	0.17 ± 0.03^b	0.27 ± 0.13^c
BGs-HAEMB	0.32 ± 0.12^c	0.49 ± 0.12^d

C

D
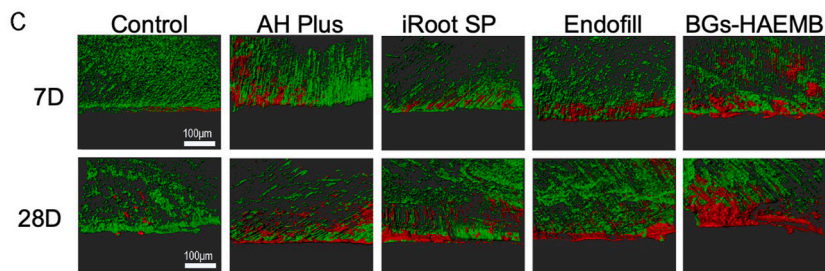
Materials	Red fluorescence ratio of *S. sanguis* at 7 and 28 days treatment ($\bar{x} \pm s$)	
	Time (Day)	
	7D	28D
Control	0.06 ± 0.04^a	0.17 ± 0.12^a
AH Plus	0.16 ± 0.03^b	0.22 ± 0.10^a
iRoot SP	0.17 ± 0.07^b	0.31 ± 0.06^b
Endofill	0.23 ± 0.04^c	0.40 ± 0.07^c
BGs-HAEMB	0.34 ± 0.6^d	0.52 ± 0.04^d

E

F
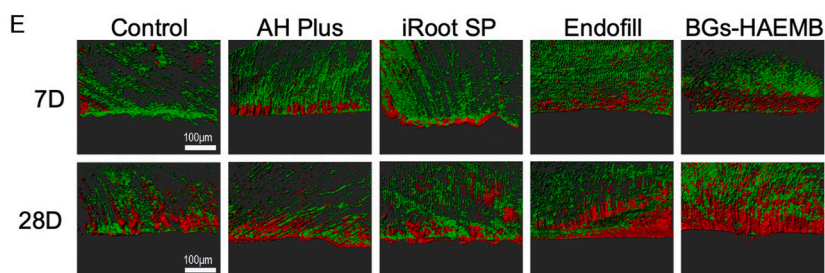
Materials	Red fluorescence ratio of *P. endodontalis* at 7 and 28 days treatment ($\bar{x} \pm s$)	
	Time (Day)	
	7D	28D
Control	0.11 ± 0.06^a	0.36 ± 0.08^a
AH Plus	0.23 ± 0.03^b	0.39 ± 0.10^a
iRoot SP	0.19 ± 0.07^b	0.41 ± 0.06^a
Endofill	0.27 ± 0.04^c	0.52 ± 0.07^b
BGs-HAEMB	0.35 ± 0.6^d	0.65 ± 0.04^c

(caption on next page)

Fig. 7. CLSM images of *E. faecalis*, *S. sanguis* and *P. endodontalis* treated with BGs-HAEMB, Endofill, AH Plus and iRoot SP for 7 and 28 days. (A, C, E) dead/live bacteria of *E. faecalis*, *S. sanguis*, *P. endodontalis* within the dentinal tubules after treatment; Scale bar = 100 μm. (B, D, F) Tables respectively showed the ratios of red fluoresce of *E. faecalis*, *S. sanguis*, *P. endodontalis* after 7- and 28-days treatment. Different letters between groups at the same time of the same strain indicated statistical differences, *P* < 0.05. (For interpretation of the references to color in this figure legend, the reader is referred to the Web version of this article.)

S. sanguinis were 3.125 μg/mL and 1.5625 μg/mL, and the MBCs of HAEMB against *E. faecalis*, *S. sanguinis*, and *P. endodontalis* were 3.125 μg/mL, 3.125 μg/mL and 1.5625 μg/mL, respectively.

3.4. Characterization of BGs-HAEMB

As shown in Fig. 1B–E, BGs-HAEMB displayed a regular spherical morphology and smooth surface with a uniform size. The average diameter of BGs-HAEMB was approximately 192 ± 1.17 nm. The successful synthesis of BGs-HAEMB was further confirmed by EDS and AFT-FTIR (Figs. S3A–E).

3.5. Antibacterial activity of BGs-HAEMB

3.5.1. ADT
The average diameters of the bacteriostatic rings against *E. faecalis*, *S. sanguis* and *P. endodontalis* are summarized in Fig. 2A and the ADT results are shown in Fig. 2B. Although variable bacteriostatic rings were presented in the Endofill, AH Plus, and ampicillin groups, no rings were observed in the BGs-HAEMB or iRoot SP groups.

3.5.2. DCT
Fig. 2C shows the DCT results of the tested materials after different sitting times. During the test period, all freshly prepared materials showed the strongest antibacterial effects (*P* < 0.05) while the antibacterial activity weakened gradually in all test groups. However, compared with Endofill, AH Plus, and iRoot SP, BGs-HAEMB exhibited the relatively strongest antibacterial effect against *E. faecalis*, *S. sanguis* and *P. endodontalis* after sitting for 14 and 28 days (*P* < 0.01).

3.6. Antibiofilm formation activity of BGs-HAEMB

CLSM images of *E. faecalis, S. sanguis,* and *P. endodontalis* biofilms that had formed for 0, 1, 7, 14, and 28 days in the presence of BGs-HAEMB, iRoot SP, AH Plus and Endofill are shown in Figs. 3A, 4A and 5A, respectively. The corresponding dead bacteria ratios are shown in Figs. 3B, 4B and 5B.

For each specific test strain, after initial inoculation of the tested materials on the surface, the ratios of red fluorescence were significantly higher (*P* < 0.01) than that in the control group, indicating that the antibiofilm formation activities were immediately effective. As the incubation time was prolonged, the proportion of dead cells increased in all experimental groups. The dead cells ratio was the highest in the BGs-HAEMB groups compared to that in the Endofill, AH Plus and iRoot SP groups at 7, 14, and 28 days, indicating that its effect on the inhibition of microorganisms' biofilm formation was the strongest and lasted (*P* < 0.01).

3.7. Activity of BGs-HAEMB against bacterial biofilm formation in experimental dentinal tubules

3.7.1. SEM evaluations
The presence of microorganism in the dentinal tubules was verified by SEM (Fig. S4). No visible microorganisms or dentin debris were observed inside the dentinal tubules (Fig. S4A). After inoculation and 4 weeks of incubation, biofilm-like structures were observed both on the surface of the root canal wall and invading into the dentinal tubules (Fig. S4B).

E. faecalis, *S. sanguis*, and *P. endodontalis* biofilms treated with BGs-HAEMB, Endofill, AH Plus and iRoot SP were observed by SEM (Fig. 6A–C). After 7 days or 28 days of treatment, the number of bacteria substantially decreased in all experimental groups. Compared to the Endofill, AH Plus and iRoot SP groups, almost no bacteria were observed on the surface of the root canal wall in the BGs-HAEMB group. In addition, the biofilm-like structures were destroyed, and the majority of the remaining bacterial cells displayed a shrunken, inconsistent, and even fractured surface.

3.7.2. Colony counts
After 7 days or 28 days of treatment, the residual colony counts of *E. faecalis*, *S. sanguis* and *P. endodontalis* decreased in all experimental groups (Fig. 6D). Notably, the residual colony counts of each specific tested strain in the BGs-HAEMB group were the lowest compared to those in the other three experimental groups (*P* < 0.05).

3.7.3. CLSM evaluations
CLSM images of *E. faecalis, S. sanguis*, and *P. endodontalis* in the experimental dentinal tubules treated with BGs-HAEMB, Endofill, AH Plus, and iRoot SP and the corresponding dead bacteria proportions are shown in Fig. 7.

After 7 days of treatment, compared to the control groups, the intensity of red fluorescence in each experimental group significantly
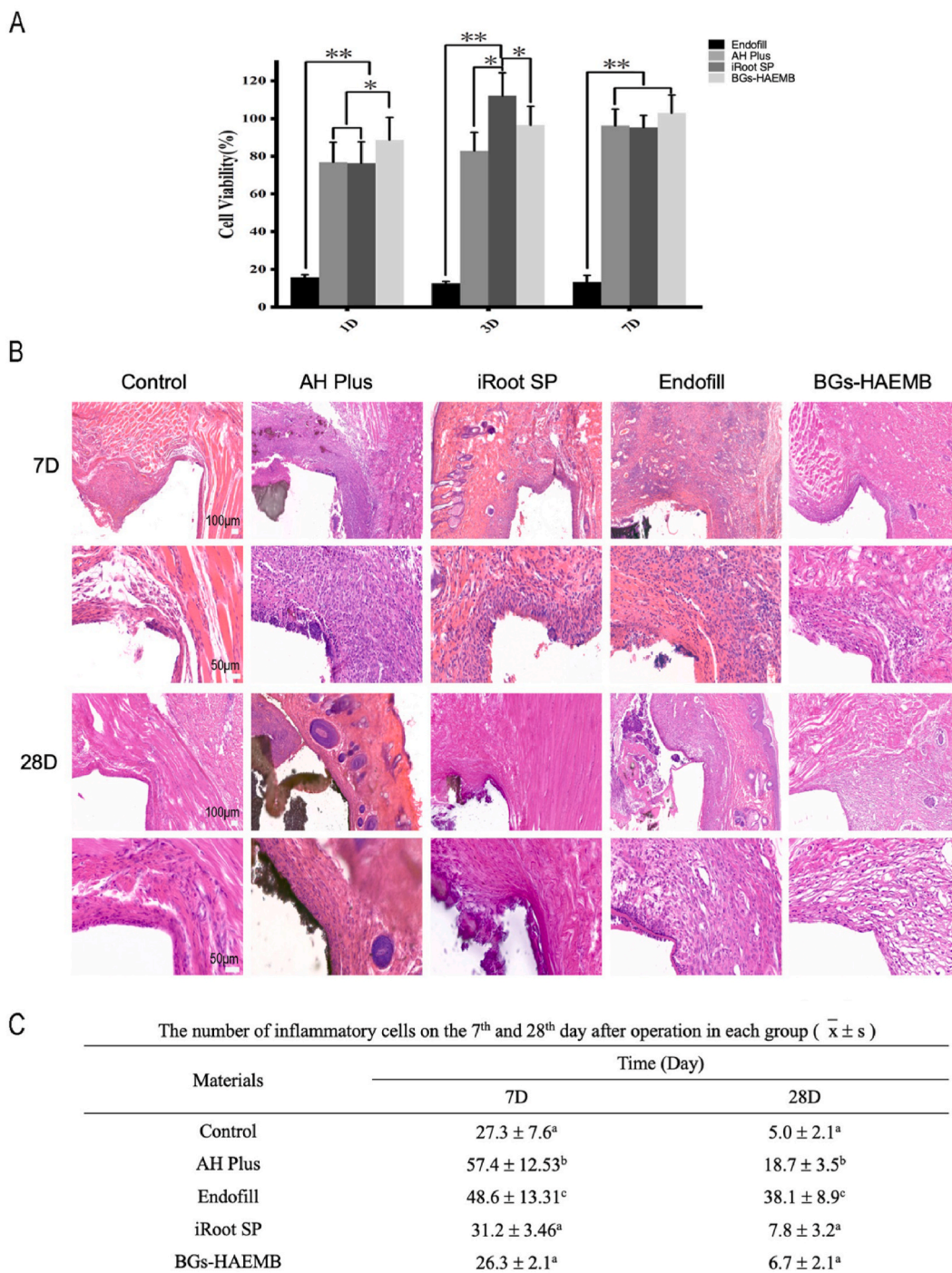
Fig. 8. *In vitro* cytotoxicity and *in vivo* biocompatibility of BGs-HAEMB, Endofill, AH Plus, iRoot SP. (A) RGR of L929 cell after incubation in extract of the four tested materials for 1, 3 and 7 days, $^*P < 0.05$, $^{**}P < 0.01$. (B). H&E staining of subcutaneous tissues after implantation of the four tested materials for 7 and 28 days. (C) Table showing the number of inflammatory cell infiltration. At the same time, different letters indicate a statistical difference between the groups, $P < 0.05$.

increased except for that in the AH Plus-treated *E. faecalis* group ($P < 0.05$). Compared to that after 7 days of treatment, a higher intensity of red fluorescence was observed in each group after treatment for 28 days ($P < 0.05$). However, for each specific tested strain, only the BGs-HAEMB and Endofill groups showed significantly higher red fluorescence ratios than the control groups ($P < 0.05$). For each tested bacteria, BGs-HAEMB killed the most microorganism among all the experimental groups, regardless of treatment for 7 days or 28 days ($P < 0.05$).

3.8. *In vitro cytotoxicity of BGs-HAEMB extract*

The *in vitro* toxicity of BGs-HAEMB, Endofill, AH Plus and iRoot SP extracts to L929 cells was assessed and shown in Fig. 8A.

After exposure to the extracts for 1, 3 and 7 days, apart from the Endofill groups (RGRs = 12.5–15.7%, Grade 4), the cell viability in the other treated groups was apparently not reduced and showed a RGR ranging from approximately 76.3%–112%, attributed to Grade 0/1 ($P < 0.05$). In addition, the BGs-HAEMB-treated groups showed a relatively high and stable RGRs ranging from 88.6% to 102.9% (Grade 0/1) after 1, 3, and 7 days of exposure.

3.9. *In vivo biocompatibility of BGs-HAEMB*

After surgery, no obvious post-operation complications of the animals were observed in all experimental groups.

The *in vivo* biocompatibility of BGs-HAEMB, Endofill, AH Plus and iRoot SP was evaluated. H&E staining images and the quantitative analysis of the inflammatory cells are shown in Fig. 8B and C. After 7 and 28 days, more inflammatory cell infiltration was observed in both the AH Plus and Endofill groups than in the iRoot SP and BGs-HAEMB groups ($P < 0.05$). The number of infiltrated inflammatory cells in the BGs-HAEMB and iRoot SP groups showed no significant difference compared to the control group ($P < 0.05$). More importantly, after 28 days of implantation, the inflammatory grade in BGs-HAEMB treated group was assessed as Grade I, in which the average numbers of inflammatory cells (6.7 ± 2.1) were less than 25.

4. Discussion

The persistence of endodontic pathogens and their biofilms within endodontically treated root canal systems is one of the major contributors to the failure of RCT and increases the incidence of reinfection [36]. *E. faecalis* is the most common microorganism isolated from infected root canal systems, with a prevalence of up to 77% [37]. *E. faecalis* can invade dentinal tubules, form biofilms and withstand extreme environments after thorough root canal mechanical-chemical disinfection treatments and the application of drug sealing techniques [38]. This pathogen has also shown resistance to common antimicrobials by undergoing mutations or acquiring resistance genes from other bacteria, leading to difficulty in its elimination [39]. *S. sanguis* and *P. endodontalis* are highly prevalent in apical lesions and play a critical role in the development of endodontic diseases [9,40]. Therefore, *E. faecalis*, *S. sanguis* and *P. endodontalis* were selected as the test strains in this study. Mechanical instrumentation and chemical disinfection are the major strategies for microorganism control [4]. Due to the anatomical complexity of the root canal system and the relative unsustainable efficacy of irrigants and intracanal medication, the application of endodontic sealers not only enhances the leakproofness of root canal filling but also plays a potentially persistent and indispensable role in the elimination of microbes from root canal systems [41]. Presently used endodontic sealers such as Endofill, AH Plus and iRoot SP show strong antibacterial effects against specific endodontic pathogens, but their antibacterial effects decrease rapidly over time [42]. In addition, the proinflammatory effect and relatively low biocompatibility of AH Plus and Endofill further limit their clinical application [43,44]. Therefore, it is necessary to develop an alternative biomaterial with effective and prolonged antibacterial effects against endodontic pathogens but with lower cytotoxicity and better biocompatibility. BGs and QAMs have shown antibacterial effects against oral pathogens and therefore have become an alternative in the development of intracanal medications [26,31]. In this study, we synthesized QAPM-grafted BGs, namely, BGs-HAEMB, which exhibited long-term antibacterial effects against *E. faecalis*, *S. sanguis* and *P. endodontalis* and showed relatively low cytotoxicity *in vitro* and supreme biocompatibility *in vivo* compared to Endofill, AH Plus and iRoot SP, representing a promising adjuvant for the development of new endodontic sealers.

The synthesis and screening procedures of the target biomaterials were different from routine physical mixing. In the current study, two materials with distinct properties, BG particles and QAMs, were covalently grafted together via a two-step approach, and yielded a novel biomaterial with a prolonged antibacterial effect against endodontic bacteria and made the functional group (QAPM) more stable.

A smaller particle size contributes to increasing antibacterial effects and promoting penetration into dentinal tubules [45]. Hence, BGs with a diameter of approximately 181 nm were selected in this study. Moreover, the QAMs with an N-ACL of 16 showed the lowest MICs and MBCs against *E. faecalis*, *S. sanguis* and *P. endodontalis* and were selected for the final grafting. Generally, an increase in the N-ACL of QAMs can increase their antibacterial effect because the long chains can extend into bacterial biofilms and destroy the biofilm integrity [46,47]. Consistently, we found that as the N-ACL increased from 3 to 16, the antibacterial ability of the QAMs increased. However, at an N-ACL of 18, the antibacterial ability of OAEMB weakened, which may be associated with its special structure. The nitrogen alkyl chain can bend or curl up when it is too long, covering the positively charged QAM group, blocking the electrostatic interactions with the bacteria, and reducing antibacterial ability. In addition, the antibacterial mechanism of the QAMs is another consideration in their selection. The antibacterial effects of short-chain QAMs mainly depend on the interaction between the self-carried cations of the QAM and the negatively charged bacterial cell membrane, resulting in the destruction of membrane function and alterations to the essential ion balance. However, long-chain QAMs show primarily charge-based bactericidal effects, as mentioned

previously, and penetrate deep into the bacterial cell membrane, resulting in physical damage and increasing antibacterial activity [48]. Above all, The BGs-HAEMB based on HAEMB (N-ACL = 16) was selected for follow-up studies.

The most important properties of an ideal endodontic sealer are effective antibacterial activity and good biocompatibility. To measure the properties of BGs-HAEMB, three endodontic sealers commonly used in the clinic (AH Plus, iRoot SP and Endofill) were chosen as controls in this study. The results showed that the BGs-HAEMB exhibited a relatively stronger antibacterial effect as well as better biocompatibility.

The elimination of infection within the root canal systems contributes greatly to the success of endodontic treatment. In this study, BGs-HAEMB showed significant and long-term antibacterial effects against the planktonic form of the tested strains. Specifically, the DCT results showed that BGs-HAEMB exhibited a remarkably continuous antibacterial effect after 28 days, indicating its future use in the development of endodontic sealers. In the current study, we also found that there was antibacterial ring in the ADT after treatment with BGs-HAEMB, verifying that contact inhibition was potentially involved in the antibacterial mechanism. Microbial biofilms, strongly related to drug resistance, play a critical role in persistent root canal infections and the failure of endodontic treatment [38]. In the current study, we found that the antibacterial effects of Endofill AH Plus and iRoot SP on biofilm formation by the tested strains were weakened or disappeared with the extension of curing time, whereas BGs-HAEMB showed a continuous antibiofilm formation effect even after 28 days of curing, supporting its potential use for the development of a long-term antibacterial endodontic sealer. Eliminating microorganisms residing in dentinal tubules leads to the success of endodontic treatment [49]. In the present study, the SEM and CLSM results indicated that BGs-HAEMB exhibited a superior antibacterial effect, both on the surface of the root canal wall and in the deep dentinal layers, against the biofilms of the tested strain in dentinal tubules in a time-dependent manner.

In addition to antibacterial activity, biocompatibility is another crucial factor of endodontic sealers that needs to be thoroughly considered for clinical application, especially in the cases of open apex, root resorption, foramen enlargement and root perforation, in which there is a high risk of tissue inflammation when endodontic sealers are extruded [50]. The present study evaluated the toxicity of BGs-HAEMB to L929 cells. The BGs-HAEMB-treated groups showed a relatively high and stable RGRs ranging from 88.6% to 102.9% (Grade 0/1) after 1, 3, and 7 days of exposure, suggesting the low cytotoxicity of BGs-HAEMB and meeting the qualification criteria [34]. In addition, after implantation for 7 and 28 days *in vivo*, BGs-HAEMB showed favorable biocompatibility similar to that of iRoot SP and better than that of AH Plus and Endofill.

According to previous reports, Endofill was suggested to have the strongest antibacterial effect among the current clinical endodontic sealers [51]. The antibacterial effect of Endofill is mainly associated with the release of eugenol and Zn^{2+}. Therefore, as the release of eugenol and Zn^{2+} during the curing process decreased, the antibacterial effect gradually weakened, which was confirmed in our study and was consistent with the results in other studies [52]. However, it still presented the highest cytotoxicity and inflammatory reactions among the tested materials at 7 and 28 days. Similar to Endofill, AH Plus exerts antibacterial effects by releasing formaldehyde and bisphenol A-diglycidyl ether. Formaldehyde can penetrate the bacterial cell membrane and inhibit metabolism by reacting with cytoplasmic proteins, RNA, and DNA. Moreover, during this process, the unreacted monomers induce cytotoxicity and inflammatory reaction in the surrounding tissue [43]. Therefore, in the current study, owing to the decreased release of formaldehyde and bisphenol A-diglycidyl ether through the curing process, decreased (from moderate to low) cytotoxicity and inflammatory reactions were observed with the AH Plus samples during the 1–7 day *in vitro* evaluation and the 7–28 day *in vivo* examination. The antibacterial effect of AH Plus decreased substantially to a level similar to that of the control groups. In the present study, although it presented unsustainable antibacterial effects, iRoot SP showed long-term effects, low cytotoxicity and few inflammatory reactions, similar to those of BGs-HAEMB. The superior biocompatibility and osteogenic potential of iRoot SP has been well documented due to the release of Ca^{2+} [53]. However, balancing the antibacterial effects and biocompatibility of an endodontic sealer remains a great challenge. In this study, the synthesized BGs-HAEMB preserved the superior antibacterial effect of the loaded QAPM [54]. BGs are verified more reactive in aqueous media and their reactivity is correlated with higher surface area [27]. Therefore, due to nanosized particle, the BGs should exhibit an antibacterial ability. However, in the present investigation, a series of quaternary ammonium methacrylate salts (QAMs) were grafted to the surface of BGs to act as the main antibacterial component. The antibacterial effect of the final product was supposed to be mainly determined by the nitrogen alkyl chain lengths (N-ACLs) of the QAM monomers, which had been proved according to the present results. Moreover, BGs can release ions, which interact with the bacterial membrane, reduce the activity of related enzymes within and outside the bacterial membrane, increase the pH, and affect the integrity of the membrane, resulting in a strong antibacterial effect [55,56]. Consider the factors associated with BG particles antibacterial effects, the surface area, the pH, and the antibacterial effect of BG particles should also be considered and assessed in our future investigation. In addition, BGs can form complex ionic bonds with dentin, which enhances its antibacterial activity [57,58] and showed relatively stable, long-term, and effective antibacterial activity during the tested period (28 days). Moreover, the low cytotoxicity and excellent biocompatibility of BGs-HAEMB can be attributed to its components. The broadly distributed bonding network between the oxygen and silicon atoms endows BGs with a high content of silica for good bioactivity [59]. The bioactivity of the BGs was also confirmed by promoting the odontogenic differentiation of human dental pulp stem cells and stimulating the growth and osteogenic differentiation of human primary osteoblasts [60]. Our results demonstrated that BGs-HAEMB sustained high bioactivity, similar to other BGs.

However, some caution should be taken when interpreting the data from the current study. To further develop BGs-HAEMB as a clinically used endodontic sealer, more investigations should be performed on its fluidity, curing time and other properties.

5. Conclusion

The final synthetic material, BGs-HAEMB, exerted a long-term and stable antibacterial effect. The remarkable biocompatibility of BGs-HAEMB *in vitro* and *in vivo* confirmed its possible clinical application. Taken together, these data indicate that the synthetic

nanomaterial BGs-HAEMB has potential as a next-generation substrate material for the development of a novel endodontic sealer to supplement the control of endodontic infections.

Funding

Ethical approval

Approved.

Data availability statement

Data will be made available on request directly to the corresponding author.

CRediT authorship contribution statement

Jin Liu: Writing – original draft, Visualization, Validation, Software, Methodology, Data curation. **Haoze Wu:** Writing – original draft, Validation, Formal analysis, Data curation. **Jun Qiu:** Writing – original draft, Validation, Formal analysis, Data curation, Conceptualization. **Sirui Yang:** Software, Resources, Data curation. **Doudou Xiang:** Software, Resources, Data curation. **Xinhua Zhang:** Software, Resources, Data curation. **Jinxin Kuang:** Software, Resources, Data curation. **Min Xiao:** Writing – review & editing, Supervision, Resources, Project administration, Funding acquisition. **Qing Yu:** Writing – review & editing, Supervision, Resources, Project administration, Funding acquisition. **Xiaogang Cheng:** Writing – review & editing, Project administration, Funding acquisition, Conceptualization.

Declaration of competing interest

The authors declare that they have no known competing financial interests or personal relationships that could have appeared to influence the work reported in this paper.

Acknowledgments

Appendix A. Supplementary data

Supplementary data to this article can be found online at https://doi.org/10.1016/j.heliyon.2024.e28266.

References

[1] D. Ricucci, J.F. Siqueira Jr., Biofilms and apical periodontitis: study of prevalence and association with clinical and histopathologic findings, J. Endod. 36 (8) (2010) 1277–1288.
[2] X. Luo, Q. Wan, L. Cheng, R. Xu, Mechanisms of bone remodeling and therapeutic strategies in chronic apical periodontitis, Front. Cell. Infect. Microbiol. 12 (2022) 908859.
[3] S.A. Niazi, A. Bakhsh, Association between endodontic infection, its treatment and systemic health: a narrative review, Medicina 58 (7) (2022).
[4] Q. Yu, [Scavenging strategy for root canal infection], Zhonghua Kou Qiang Yi Xue Za Zhi 53 (6) (2018) 381–385.
[5] P.N. Nair, Pathogenesis of apical periodontitis and the causes of endodontic failures, Crit. Rev. Oral Biol. Med. 15 (6) (2004) 348–381.
[6] J.F. Siqueira Jr., Rocas IN, Ricucci D, Hulsmann M: causes and management of post-treatment apical periodontitis, Br. Dent. J. 216 (6) (2014) 305–312.
[7] M. Barbosa-Ribeiro, R. Arruda-Vasconcelos, L.M. Louzada, D.G. Dos Santos, F.D. Andreote, B. Gomes, Microbiological analysis of endodontically treated teeth with apical periodontitis before and after endodontic retreatment, Clin. Oral Invest. 25 (4) (2021) 2017–2027.
[8] R.X. Lins, A. de Oliveira Andrade, R. Hirata Junior, M.J. Wilson, M.A. Lewis, D.W. Williams, R.A. Fidel, Antimicrobial resistance and virulence traits of Enterococcus faecalis from primary endodontic infections, J. Dent. 41 (9) (2013) 779–786.
[9] N. Ma, D. Yang, H. Okamura, J. Teramachi, T. Hasegawa, L. Qiu, T. Haneji, Involvement of interleukin-23 induced by Porphyromonas endodontalis lipopolysaccharide in osteoclastogenesis, Mol. Med. Rep. 15 (2) (2017) 559–566.
[10] A. Khandelwal, K. Janani, K. Teja, J. Jose, G. Battineni, F. Riccitiello, A. Valletta, A. Palanivelu, G. Spagnuolo, Periapical healing following root canal treatment using different endodontic sealers: a systematic review, BioMed Res. Int. 2022 (2022) 3569281.
[11] F.F.E. Torres, J.M. Guerreiro-Tanomaru, R. Bosso-Martelo, C.G. Espir, J. Camilleri, M. Tanomaru-Filho, Solubility, porosity, dimensional and volumetric change of endodontic sealers, Braz. Dent. J. 30 (4) (2019) 368–373.
[12] M. Ruiz-Linares, M.E. Bailon-Sanchez, P. Baca, M. Valderrama, C.M. Ferrer-Luque, Physical properties of AH Plus with chlorhexidine and cetrimide, J. Endod. 39 (12) (2013) 1611–1614.

[13] C.M. Giacomino, J.A. Wealleans, N. Kuhn, A. Diogenes, Comparative biocompatibility and osteogenic potential of two bioceramic sealers, J. Endod. 45 (1) (2019) 51–56.
[14] W. Zhang, B. Peng, Tissue reactions after subcutaneous and intraosseous implantation of iRoot SP, MTA and AH Plus, Dent. Mater. J. 34 (6) (2015) 774–780.
[15] B. Gandhi, R. Halebathi-Gowdra, Comparative evaluation of the apical sealing ability of a ceramic based sealer and MTA as root-end filling materials - an in-vitro study, J Clin Exp Dent 9 (7) (2017) e901–e905.
[16] W. Qu, W. Bai, Y.H. Liang, X.J. Gao, Influence of warm vertical compaction technique on physical properties of root canal sealers, J. Endod. 42 (12) (2016) 1829–1833.
[17] M. Lim, C. Jung, D.H. Shin, Y.B. Cho, M. Song, Calcium silicate-based root canal sealers: a literature review, Restor Dent Endod 45 (3) (2020) e35.
[18] W. Song, S. Ge, Application of antimicrobial nanoparticles in dentistry, Molecules 24 (6) (2019).
[19] B.L. Correia, A. Gomes, R. Noites, J.M.F. Ferreira, A.S. Duarte, New and efficient bioactive glass compositions for controlling endodontic pathogens, Nanomaterials 12 (9) (2022).
[20] Z. Wu, J. Bai, G. Ge, T. Wang, S. Feng, Q. Ma, X. Liang, W. Li, W. Zhang, Y. Xu, et al., Regulating macrophage polarization in high glucose microenvironment using lithium-modified bioglass-hydrogel for diabetic bone regeneration, Adv. Healthcare Mater. 11 (13) (2022) e2200298.
[21] J. Bauer, E.S.A. Silva, E.M. Carvalho, P.V.C. Ferreira, C.N. Carvalho, A.P. Manso, R.M. Carvalho, Dentin pretreatment with 45S5 and niobophosphate bioactive glass: effects on pH, antibacterial, mechanical properties of the interface and microtensile bond strength, J. Mech. Behav. Biomed. Mater. 90 (2019) 374–380.
[22] P. Ranganathan, V. Sugumaran, B. Purushothaman, A.R. Rajendran, B. Subramanian, Rapidly derived equimolar Ca: P phasic bioactive glass infused flexible gelatin multi-functional scaffolds – a promising tissue engineering, J. Mech. Behav. Biomed. Mater. 150 (2024) 106264.
[23] H. Palza Cordero, R. Castro Cid, M. Diaz Dosque, R. Cabello Ibacache, P. Palma Fluxa, Li-doped bioglass(R) 45S5 for potential treatment of prevalent oral diseases, J. Dent. 105 (2021) 103575.
[24] L. Wang, W. Xu, Y. Chen, J. Wang, Alveolar bone repair of rhesus monkeys by using BMP-2 gene and mesenchymal stem cells loaded three-dimensional printed bioglass scaffold, Sci. Rep. 9 (1) (2019) 18175.
[25] R. Ramadoss, R. Padmanaban, B. Subramanian, Role of bioglass in enamel remineralization: existing strategies and future prospects-A narrative review, J. Biomed. Mater. Res. B Appl. Biomater. 110 (1) (2022) 45–66.
[26] G. Huang, S.Y. Liu, J.L. Wu, D. Qiu, Y.M. Dong, A novel bioactive glass-based root canal sealer in endodontics, J. Dent. Sci. 17 (1) (2022) 217–224.
[27] M. Montazerian, F. Baino, E. Fiume, C. Migneco, A. Alaghmandfard, O. Sedighi, A.V. DeCeanne, C.J. Wilkinson, J.C. Mauro, Glass-ceramics in dentistry: fundamentals, technologies, experimental techniques, applications, and open issues, Prog. Mater. Sci. 132 (2023) 101023.
[28] X. Fu, Y. Zhang, X. Jia, Y. Wang, T. Chen, Research progress on typical quaternary ammonium salt polymers, Molecules 27 (4) (2022).
[29] X. Shen, B. Gao, K. Guo, C. Yu, Q. Yue, PAC-PDMDAAC pretreatment of typical natural organic matter mixtures: ultrafiltration membrane fouling control and mechanisms, Sci. Total Environ. 694 (2019) 133816.
[30] A.C. Maia, A. Mangabeira, R. Vieira, A.A. Neves, R.T. Lopes, T.M. Pires, G.M. Viana, L.M. Cabral, L.M. Cavalcante, M.B. Portela, Experimental composites containing quaternary ammonium methacrylates reduce demineralization at enamel-restoration margins after cariogenic challenge, Dent. Mater. 35 (8) (2019) e175–e183.
[31] A.S. Khan, S. Ur Rehman, Y.K. AlMaimouni, S. Ahmad, M. Khan, M. Ashiq, Bibliometric analysis of literature published on antibacterial dental adhesive from 1996-2020, Polymers 12 (12) (2020).
[32] D. Kesler Shvero, I. Abramovitz, N. Zaltsman, M. Perez Davidi, E.I. Weiss, N. Beyth, Towards antibacterial endodontic sealers using quaternary ammonium nanoparticles, Int. Endod. J. 46 (8) (2013) 747–754.
[33] J. Ma, Z. Wang, Y. Shen, M. Haapasalo, A new noninvasive model to study the effectiveness of dentin disinfection by using confocal laser scanning microscopy, J. Endod. 37 (10) (2011) 1380–1385.
[34] A. Unsworth, Proceedings of the institution of mechanical engineers, Part H: Journal of Engineering in Medicine, Proc. Inst. Mech. Eng. H 230 (1) (2016), 3-3.
[35] S. Shahi, S. Rahimi, H.R. Yavari, H. Mokhtari, L. Roshangar, M.M. Abasi, S. Sattari, M. Abdolrahimi, Effect of mineral trioxide aggregates and Portland cements on inflammatory cells, J. Endod. 36 (5) (2010) 899–903.
[36] M. Dioguardi, C. Quarta, M. Alovisi, V. Crincoli, R. Aiuto, R. Crippa, F. Angiero, E. Laneve, D. Sovereto, A. De Lillo, et al., Microbial association with genus Actinomyces in primary and secondary endodontic lesions, review, Antibiotics 9 (8) (2020).
[37] C.H. Stuart, S.A. Schwartz, T.J. Beeson, C.B. Owatz, Enterococcus faecalis: its role in root canal treatment failure and current concepts in retreatment, J. Endod. 32 (2) (2006) 93–98.
[38] D.C.M. Todea, R.E. Luca, C.A. Balabuc, M.I. Miron, C. Locovei, D.E. Mocuta, Scanning electron microscopy evaluation of the root canal morphology after Er:YAG laser irradiation, Rom. J. Morphol. Embryol. 59 (1) (2018) 269–275.
[39] S. Wu, Y. Liu, H. Zhang, L. Lei, The susceptibility to calcium hydroxide modulated by the essential walR gene reveals the role for Enterococcus faecalis biofilm aggregation, J. Endod. 45 (3) (2019) 295–301 e292.
[40] L. Hong, J. Hai, H. Yan-Yan, Y. Shenghui, H. Benxiang, [Colonization of Porphyromonas endodontalis in primary and secondary endodontic infections], Hua xi kou qiang yi xue za zhi 33 (1) (2015) 88–92.
[41] E. AlShwaimi, D. Bogari, R. Ajaj, S. Al-Shahrani, K. Almas, A. Majeed, In vitro antimicrobial effectiveness of root canal sealers against Enterococcus faecalis: a systematic review, J. Endod. 42 (11) (2016) 1588–1597.
[42] H.M. Zhou, T.F. Du, Y. Shen, Z.J. Wang, Y.F. Zheng, M. Haapasalo, In vitro cytotoxicity of calcium silicate-containing endodontic sealers, J. Endod. 41 (1) (2015) 56–61.
[43] S. Jung, S. Sielker, M.R. Hanisch, V. Libricht, E. Schafer, T. Dammaschke, Cytotoxic effects of four different root canal sealers on human osteoblasts, PLoS One 13 (3) (2018) e0194467.
[44] L. Teixeira, F.G. Basso, J. Hebling, C.A.S. Costa, G.G. Mori, Y.T.C. Silva-Sousa, C.F. Oliveira, Cytotoxicity evaluation of root canal sealers using an in vitro experimental model with roots, Braz. Dent. J. 28 (2) (2017) 165–171.
[45] W. Cao, Y. Zhang, X. Wang, Y. Chen, Q. Li, X. Xing, Y. Xiao, X. Peng, Z. Ye, Development of a novel resin-based dental material with dual biocidal modes and sustained release of Ag(+) ions based on photocurable core-shell AgBr/cationic polymer nanocomposites, J. Mater. Sci. Mater. Med. 28 (7) (2017) 103.
[46] P. Makvandi, R. Jamaledin, M. Jabbari, N. Nikfarjam, A. Borzacchiello, Antibacterial quaternary ammonium compounds in dental materials: a systematic review, Dent. Mater. 34 (6) (2018) 851–867.
[47] S. Imazato, T. Kohno, R. Tsuboi, P. Thongthai, H.H. Xu, H. Kitagawa, Cutting-edge filler technologies to release bio-active components for restorative and preventive dentistry, Dent. Mater. J. 39 (1) (2020) 69–79.
[48] Y. Jiao, F.R. Tay, L.N. Niu, J.H. Chen, Advancing antimicrobial strategies for managing oral biofilm infections, Int. J. Oral Sci. 11 (3) (2019) 28.
[49] Z. Wang, Y. Shen, M. Haapasalo, Dentin extends the antibacterial effect of endodontic sealers against Enterococcus faecalis biofilms, J. Endod. 40 (4) (2014) 505–508.
[50] J.F. Siqueira Junior, I.D.N. Rocas, M.F. Marceliano-Alves, A.R. Perez, D. Ricucci, Unprepared root canal surface areas: causes, clinical implications, and therapeutic strategies, Braz. Oral Res. 32 (suppl 1) (2018) e65.
[51] R.D. Morgental, F.V. Vier-Pelisser, S.D. Oliveira, F.C. Antunes, D.M. Cogo, P.M. Kopper, Antibacterial activity of two MTA-based root canal sealers, Int. Endod. J. 44 (12) (2011) 1128–1133.
[52] F.E. Baldasso, P.M. Kopper, R.D. Morgental, L. Steier, J.A. Figueiredo, R.K. Scarparo, Biological tissue response to a new formulation of a silicone based endodontic sealer, Braz. Dent. J. 27 (6) (2016) 657–663.
[53] S.W. Chang, S.Y. Lee, S.K. Kang, K.Y. Kum, E.C. Kim, In vitro biocompatibility, inflammatory response, and osteogenic potential of 4 root canal sealers: Sealapex, Sankin apatite root sealer, MTA Fillapex, and iRoot SP root canal sealer, J. Endod. 40 (10) (2014) 1642–1648.
[54] B. Gottenbos, H.C. van der Mei, F. Klatter, P. Nieuwenhuis, H.J. Busscher, In vitro and in vivo antimicrobial activity of covalently coupled quaternary ammonium silane coatings on silicone rubber, Biomaterials 23 (6) (2002) 1417–1423.

[55] A. Clichici, G.A. Filip, M. Achim, I. Baldea, C. Cristea, G. Melinte, O. Pana, L.B. Tudoran, D. Dudea, R. Stefan, Characterization and in vitro biocompatibility of two new bioglasses for application in dental medicine-A preliminary study, Materials 15 (24) (2022).

[56] V. Farano, J.C. Maurin, N. Attik, P. Jackson, B. Grosgogeat, K. Gritsch, Sol-gel bioglasses in dental and periodontal regeneration: a systematic review, J. Biomed. Mater. Res. B Appl. Biomater. 107 (4) (2019) 1210–1227.

[57] F.A. Shah, Fluoride-containing bioactive glasses: glass design, structure, bioactivity, cellular interactions, and recent developments, Mater. Sci. Eng., C 58 (2016) 1279–1289.

[58] R. Riju Chandran, S. Chitra, S. Vijayakumari, P. Bargavi, S. Balakumar, Cognizing the crystallization aspects of NaCaPO4 concomitant 53S bioactive-structures and their imprints in in vitro bio-mineralization, New J. Chem. 45 (34) (2021) 15350–15362.

[59] S. Labbaf, O. Tsigkou, K.H. Muller, M.M. Stevens, A.E. Porter, J.R. Jones, Spherical bioactive glass particles and their interaction with human mesenchymal stem cells in vitro, Biomaterials 32 (4) (2011) 1010–1018.

[60] Y.L. Li, Q.M. Liang, C. Lin, X. Li, X.F. Chen, Q. Hu, Facile synthesis and characterization of novel rapid-setting spherical sub-micron bioactive glasses cements and their biocompatibility in vitro, Mat Sci Eng C-Mater 75 (2017) 646–652.